UNIVERSIDAD NACIONAL DE COLOMBIA
SEDE MEDELLÍN
FACULTAD DE MINAS

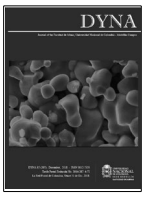

DYNA
http://dyna.medellin.unal.edu.co/

Corrosion resistance and tribological behavior of WS_2-Ti coatings by Ti cathode power changes in magnetron co-sputtering

Jhonattan de la Roche-Yepes [a], Juan Manuel González [b,c], Elizabeth Restrepo-Parra [a] & Héctor Sánchez-Sthepa [c]

[a] *Laboratorio de Física del Plasma, PCM Computational Applications, Universidad Nacional de Colombia Sede Manizales, Manizales, Colombia, jdey@unal.edu.co, erestrepopa@unal.edu.co*
[b] *Ingeniería de Superficies y Manufactura Aditiva, Centro de Ingeniería y Desarrollo Industrial-CIDESI, Querétaro, México. juan.gonzalez@cidesi.edu.mx*
[c] *Laboratorio de Recubrimientos Duros y Aplicaciones Industriales – RDAI, Universidad del Valle, Cali, Colombia, hector.sanchez@correounivalle.edu.co*

Received: September27th, de 2017. Received in revised form: March 10th, 2018. Accepted: July 22th, 2018

Abstract
Titanium-doped tungsten disulfide thin films (WS_2-Ti) were deposited using a DC magnetron co-sputtering on AISI 304 stainless steel and silicon substrates. Different Ti cathode power densities between 0 and 1.25 W/cm^2 were used for coating deposition. Energy-dispersive spectroscopy evidenced an increase in Ti percentage at the expense of W, as well as a sulfur deficiency. Raman spectroscopy was used to identify bands corresponding to W-S for undoped WS_2. As the material was doped, changes in crystalline structure caused W-S main bands to separate. Scratch adhesion testing showed that Ti percentage increased along with the critical load (Lc). Furthermore, adhesive failure type changed from plastic to elastic. Finally, corrosion resistance analysis using electrochemical impedance spectroscopy (EIS) showed that, at high Ti concentrations, corrosion resistance was enhanced as Ti facilitates coating densification and generates a protective layer.

Keywords: solid lubricant; TMD; Raman, EIS; doping.

Películas de WS_2-Ti producidas por magnetrón co-sputtering variando la potencia del cátodo de titanio: comportamiento tribológico y resistencia a la corrosión

Resumen
Películas delgadas de bisulfuro de tungsteno dopado con titanio fueron depositadas usando la técnica de magnetron co- sputtering DC sobre sustratos de acero inoxidable AISI 304 y Silicio. Para producir los recubrimientos, la densidad de potencia del cátodo de titanio fue variada entre 0 y 1.25 W/cm^2. Los resultados de espectroscopia de energía dispersiva muestran un incremento en el porcentaje de Ti a expensas de W, además muestra una disminución en el porcentaje de azufre. Con las medidas de espectroscopía Raman se identificaron las bandas al enlace W-S para WS_2 sin dopar. Cuando el material es dopado, los cambios en la estructura cristalina producen la separación de las principales bandas del enlace W-S. Usando la prueba de rayado dinámico, la adhesión de los recubrimientos fue estudiada, mostrando que la carga critica (Lc) incrementa con el porcentaje de Ti; además, la falla pasa de adhesiva a cohesiva con el incremento de Ti. Finalmente, la resistencia a la corrosión fue evaluada usando la técnica espectroscopia de impedancia electroquímica (EIS), y es observado que a altas cantidades de Ti, se mejora la resistencia a la corrosión debido a que el Ti facilita la densificación y genera una capa protectora.

Palabras clave: lubricante sólido; TMD; Raman; EIS; dopaje.

1. Introduction

Solid lubricant coatings have attracted significant attention in recent years, as they can drastically reduce material wear rate and surface friction in an extensive range of sliding environments [1-4]. Among different types of materials used in

How to cite: de la Roche-Yepes, J., González, J.M., Restrepo-Parra, E. and Sánchez-Sthepa, H., Corrosion resistance and tribological behavior of WS2-Ti coatings by Ti cathode power changes in magnetron co-sputtering. DYNA, 85(207), pp. 221-226, Octubre - Diciembre, 2018.

Revista DYNA, 85(207), pp. 221-226, Octubre - Diciembre, 2018, ISSN 0012-7353
DOI: http://doi.org/10.15446/dyna.v85n207.67980

solid lubricant applications, transition-metal dichalcogenides (TMDs) (sulfides, selenides or tellurides of tungsten, molybdenum and niobium) have been regarded as being of major importance for applications, including solid lubricants, in the aeronautic and aerospace industry [5]. For instance, one of the most widely used TMDs is tungsten disulfide (WS_2), due to its high thermal stability (~500 °C in air) and low friction coefficient (between 0.02 and 0.06) [6,7]. Because of these outstanding properties, WS_2 can be considered as a suitable material for applications where low friction (lubricity) at high temperatures is required [8]. On the other hand, the hexagonal structure of WS_2 comprises S-W-S atomic planes joined by covalent bonds into layers, with Van der Waals forces acting as weak interlaminar bonds that give WS_2 its lubricant behavior [6,7,9]. This structure graphite-like hexagonal layered structure makes WS_2 a very suitable material for solid lubricant applications [10]

The magnetron sputtering technique is commonly used in coatings deposition technology, since it displays greater advantages compared to other methods. These advantages result in the possibility of obtaining highly precise thicknesses and to achieve material stoichiometry control [2]. In spite of these advantages, Polcar and Cavaleiro [11] stated that the magnetron sputtering technique has disadvantages for TMD coatings production, including: a highly-disorganized structure (exhibiting low orientation in the (0002) plane); extremely high sensitivity to environmental attacks; high porosity; and poor mechanical properties. These conditions affect performance of the material when used as a lubricant. A possible alternative for improving the material deposition performance by magnetron sputtering involves doping with other metallic and/or non-metallic elements [6-8,11-14]. Such doping can increase film density, adhesion and hardness. For instance, Scharf *et al*. [6] produced and characterized Ti-doped WS_2 coatings using co-sputtering for solid lubricant applications. The team found a decrease in the friction coefficient when low Ti quantities were added to WS_2 coatings. Furthermore, the addition of small, calculated amount of Ti also decreased oxides formation in high-humidity, high-temperature applications [15,16]

An important property to analyze when materials are exposed to moisture, high temperatures and aggressive environments is corrosion resistance In nanocrystalline materials, corrosion resistance depends on several factors such as the concentration of the alloying element; production conditions; microstructure; and environmental conditions [17]. Of the few studies on WS_2-Ti, not many are dedicated to the characterization of its corrosion resistance properties. WS_2-Ti corrosion resistance characteristics can be correlated with its composition and tribological properties, such as adherence and friction coefficient.

In this study, the effect of Ti doping in WS_2 compounds was analyzed. A chemical composition, friction coefficient, adhesion, and corrosion resistance of Ti-WS_2 analysis, depending on Ti cathode power applied, was conducted. The observed properties were compared with the performance of steel and undoped WS_2.

2. Materials and methods

WS2 and Ti-doped WS2 (WS2-Ti) thin films were deposited on silicon and AISI 304 stainless steel substrates using a magnetron sputtering AJA ATC 1500 system. Coatings were produced using WS2 (99.95%) and Ti (99.99%) targets with a 2-inch diameter. The sputtering system was first pumped down to 1 x10-4 Pa. Then, an Argon-based plasma cleaning process was performed for 15 min to eliminate impurities that were not removed during the previous sample cleaning. A non-reactive atmosphere of Ar was used at a working pressure of 0.4 Pa. The WS2 cathode was maintained at a constant power of 2.5 W/cm2, whereas the power of Ti cathode was set at 0, 0.25, 0.5, 0.75, 1 and 1.25 W/cm2. The elemental composition was investigated using a Philips XL 30 TMP scanning electron microscope, applying a standard Energy Dispersive Spectroscopy-EDS technique at 20 keV and 200x.

The coatings' atomic bonds were characterized by Raman spectroscopy, using a Nicolet Almega XR visible dispersive Raman microscope which included an Olympus BX51 microscope. A 532-nm laser (green-visible) at 80% power was used. The thin films' thickness was determined using a KLA Tencor D100 profilometer, obtaining an average value of 500 nm for the films set. Scratch adhesion testing was performed using NANOVEA IBIS–Technology equipment, which includes a Rockwell C diamond indenter with a 200-µm radius, 35 N of maximum load and a distance of 2.5 mm. Corrosion resistance measurements were conducted using electrochemical impedance spectroscopy (EIS) with a Potentiostat-Galvanostat Gamry series G instrument, using 3.5 wt% NaCl as the electrolyte. A calomel electrode was used as a reference electrode, with a graphite counter electrode and the coating as the work electrode, in a range between 105 and 0.01 Hz and an open-circuit time potential of 1800 seconds. Curves obtained were analyzed using the Gamry Echem Analyst software, where polarization resistance, Rp, and the equivalent circuit were determined.

2. Results

3.1. EDS analysis

Titanium, tungsten, and sulfur sample quantifications are listed on Table 1. As expected, as the power of the Ti cathode was increased, the atomic percentage of Ti was also increased, at the expense of the W percentage. Furthermore, the %S remained approximately constant. The materials did not show the expected stoichiometry (Ti-WS_2), since %S is not exactly the sum %Ti + %W. The deficiency in %S is due to the great energy amount required by Ar^+ to impact the WS_2 cathode. According to Banerjee and Chattopadhyay [18], this high energy requirement results in an enhanced dissociation of WS_2 molecules, also reflected in the sulfur deficiency of the material.

Table 1.
Atomic percentage obtained in EDS samples analysis.

Ti Power Density (W/cm^2)	%W	%S	%Ti
0	38.13	61.87	0
0.25	37.03	62.42	0.55
0.5	34.77	61.7	3.53
0.75	32.52	61.03	6.45
1	30.89	61.01	8.1
1.25	28.25	61.7	10.05

Source: The authors

3.2. Raman analysis

Fig. 1 shows the μ-Raman spectrum for undoped samples of WS_2. In this figure, bands corresponding to W-S bonds at 352 cm^{-1} and 415 cm^{-1} were identified. These bands belong to the E_{2g} mode of W+S movement in the *x-y* plane and the A_{1g} mode of the S movement in the *z* axis [19]. Bands at 695 cm^{-1} and 805 cm^{-1} were also observed [20]; the band at 695 cm^{-1} corresponds to the O-W-O stretching mode of $WO_3 \bullet nH_2O$, and the band at 805 cm^{-1} is assigned to the asymmetric stretching mode of oxygen bridges ν_a (O-W-O) [21,22]. Finally, the band observed at 518 cm^{-1} corresponds to the vibrational mode of Si [23]. O-W-O bands exist due to the material exhibiting orientations in basal planes that are perpendicular to the substrate surface (1-type films). This orientation allows exposure of the structure's lateral faces to the environment. Then, these points exhibit activation because of the dangling bonds at cell edges [23], acting as recombination sites and centers for electrochemical corrosion [24].

Fig. 2 shows μ-Raman spectra for doped samples. It is possible to deduce from these spectra that due to the inclusion of Ti in the material, a significant change was induced in the WS_2 structure. Evidence supports this is caused by the high sensitivity of Raman spectroscopy to crystalline structure variations [25]. These changes are reflected in the disappearance of the main bands at 352 cm^{-1} and 415 cm^{-1} of the E_{2g} and A_{1g} modes. The introduction of Ti in the WS_2 lattice can block the free movement of W and S, while also inducing a phase transition. Ti doping in transition metal dichalcogenides is also responsible for structure reordering and amorphization when spinodal segregation is achieved [6, 7]. As Ti percentage increases, a steeper slope of the 200 cm^{-1} and 450 cm^{-1} bands was observed for samples deposited at a Ti cathode power density of 0.75, 1 and 1.25 W/cm^2, indicating continuous material reordering and crystallization. This was corroborated by TEM images [14], which evidenced that including titanium in the structure makes it amorphous; increasing its content leads to nanocomposite form organization of the structure.

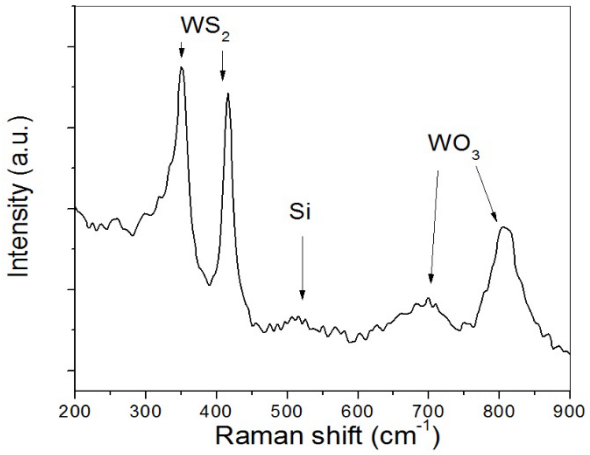

Figure 1. Raman spectra of pure WS_2.
Source: The authors

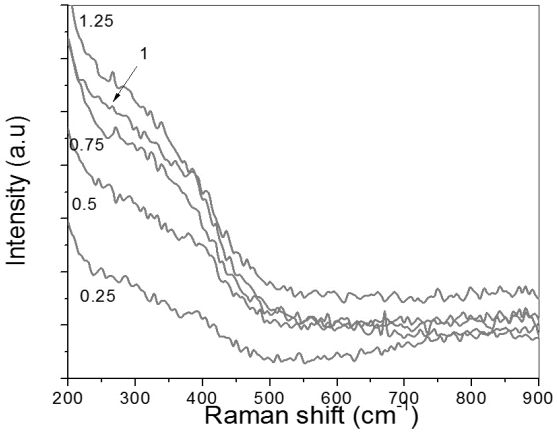

Figure 2. Raman spectra of WS_2 samples deposited at different Ti cathode power levels.
Source: The authors

3.3. Scratch test analysis

Fig. 3(a) presents the Drag coefficient (DCof) as a function of distance for undoped WS_2 samples. When a significant change occurs in the DCof-distance curve slope, a perpendicular line is traced until it intersects the load distance plot. The intersection point is then projected to the load axis to determine the critical load of the coating/substrate system. Initial fluctuations of DCof were caused during an initial stage of surface roughness polishing. As distance and load increase, the curve is stabilized. Two slope changes corresponding to adhesive and cohesive failures at critical loads of 11.5 N and 18 N respectively were observed. The image of the track obtained at 10x (Fig. 3(b)) shows a cohesive failure at 0.8 mm represented by a plastic deformation typical of laminar solids. Adhesive failures occurred at a distance of 1.3 mm, where applied load was great enough to generate film spallation.

The critical load dependence on Ti cathode power can be observed in Fig. 4(a). Abrupt changes in critical load are evidenced at 18 N and 7 N for undoped and WS_2-Ti $_{0.25\ W}$ samples, respectively. This decrease is caused by the inclusion of Ti in the WS_2 structure, which produces numerous micro-deformations and phase transitions (Fig. 4(b)). These changes contribute to stress accumulation, causing premature coating damage.

For samples deposited at power density levels greater than 0.25 W/cm^2, a progressive increase in critical load is observed. This is attributed to the following factors: (i) substrate-coating interface changes, leading to improved interaction between these and therefore increased adhesion; and (ii) an increase in hardness due to Ti doping. Changes in the coatings' characteristic failure mechanism were then observed during the scratch test, where samples exhibited buckling or spallation-type failures or a mixture of these failure types (buckling spallation) along the track (Figs. 4(b), 4(c), 4(d)). These failures were more evident as the Ti concentration increased, consistent with an increase in the fragility of coatings [26,27].

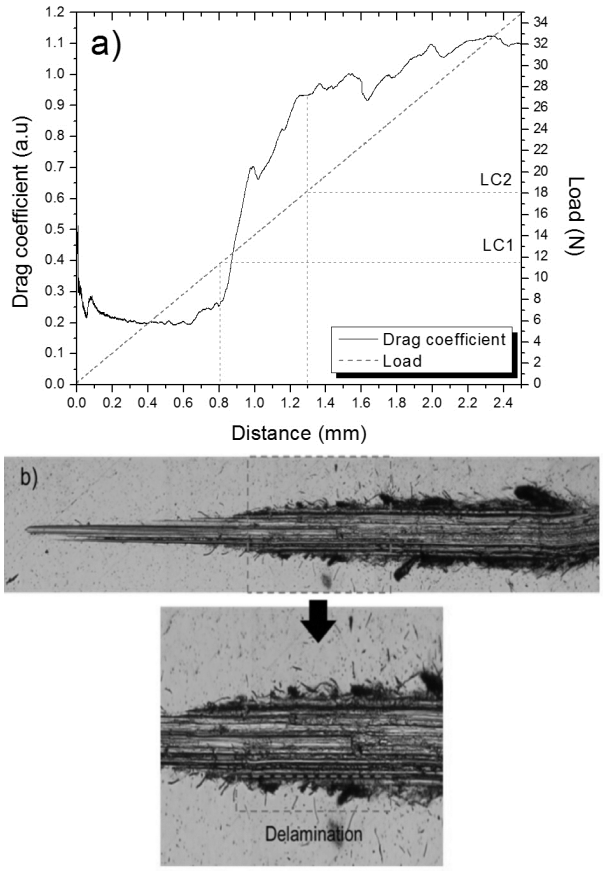

Figure 3. Scratch test (a) Drag coefficient, Load depending on the distance (b) 10x micrograph of scratch track.
Source: The authors

Nevertheless, it is important to note that critical load values for doped samples are lower than those observed for undoped coatings, indicating an apparent increase in hardness and in fragility of the material were caused as a consequence of the residual stress brought about by the dopant. These combinations of effects forced the samples to fail more easily, which decreases critical load values [26]. A similar behavior (an increase in the hardness and in the critical load of doped WS_2) is presented by Nossa and Cavaleiro [12]. They studied the mechanical properties, namely hardness and adhesion, of W-S coatings doped with nitrogen and carbon. Films were deposited using RF magnetron sputtering. Hardness and critical load of adhesion (*Lc*) values for undoped films were 0.6 ± 0.04 GPa and 5.2 N, respectively. Nevertheless, as the doping increased, the hardness and adhesion of the material increased considerably, reaching maximum values of 4.6 ± 0.3 GPa and 36.6 N for nitrogen and 5.4±0.2 GPa and 50 N for carbon. The authors attributed this behavior to the densification of the films, a phenomenon that promotes an increase in hardness and therefore an increase in critical load.

3.4. EIS analysis

Electrochemical impedance spectroscopy (EIS) testing was conducted to study the corrosion resistance behavior of steel, WS_2 and WS_2-Ti films. Results were determined by calculating polarization resistance (*Rp*) values and the equivalent circuit. Nyquist diagrams are shown in Fig. 5(a); experimentally obtained semicircles were observed, and these curves were used to carry out an adjustment using Gamry Analyst software Echem, yielding polarization resistance (*Rp*) values for each material. Resulting values are presented in Table 2.

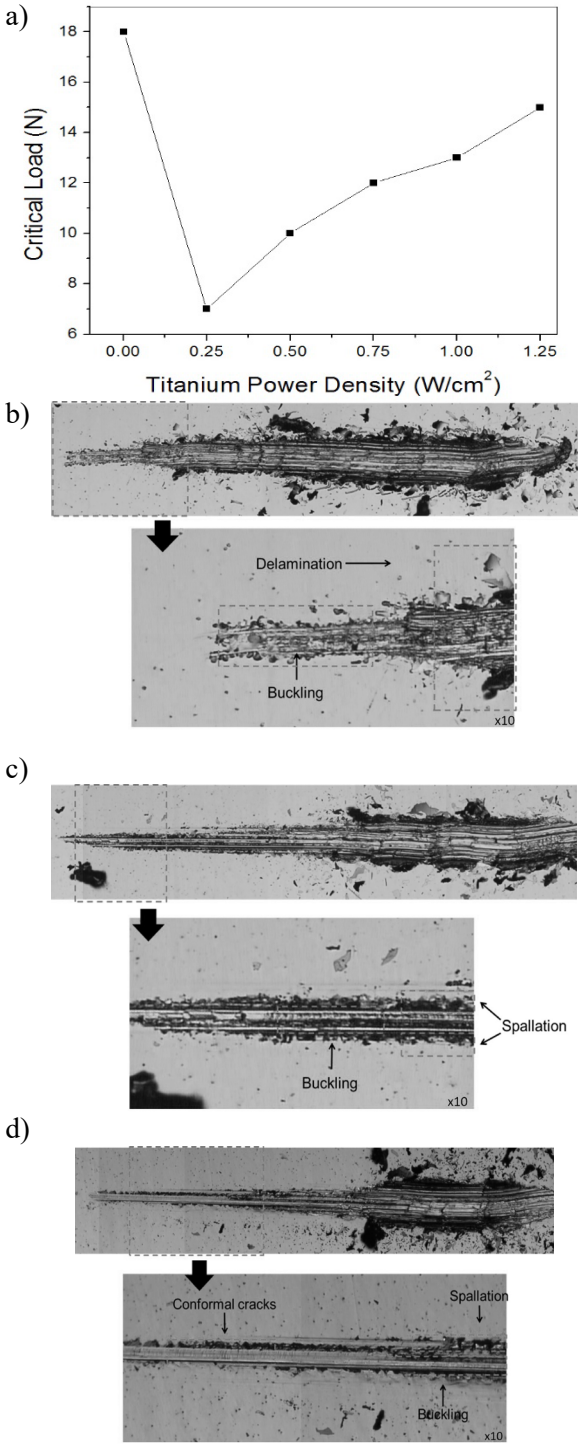

Figure 4. a) Dependence of critical load (*Lc*) on titanium cathode power density, b) 10x micrograph of scratch track WS_2-Ti $_{0.25\ W}$, c) WS_2-Ti $_{0.75\ W}$ and d) WS_2-Ti $_{1.25\ W}$.
Source: The authors

Table 2.
Rp values of steel, WS_2 and WS_2-Ti (x)

Sample	Polarization Resistance -R_P (KΩ)
AISI 304 steel	5.64±0.07
WS_2	17.34±0.16
WS_2-Ti 0.25	3.68±0.04
WS_2-Ti 0.5	15.88±0.14
WS_2-Ti 0.75	23.97±0.17
WS_2-Ti 1	34.74±0.35
WS_2-Ti 1.25	50.84±0.50

Source: The authors

The fitting was obtained from an equivalent circuit included in the software database. For these samples, the fitting was performed using a circuit containing a CPE (constant phase element), as shown in Fig. 5(b). The circuit is composed of *Ru* and *Rp* resistances, where *Rp* is parallel with an element that can work as a resistor or capacitor (CPE), which works here as a capacitor, completing a basic circuit impedance. The obtained *Rp* values showed low dispersion levels, as did the values for *Ru*, which corresponds to the resistance of a 3.5% NaCl solution with an average value of 26.67 ± 3.14 Ω [28, 29]. The low dispersion results are indicators of the validity of the results and the quality of the prepared solution.

As evidenced by the *Rp* values, the increase in corrosion resistance of steel following the addition of a WS_2 layer was observed; this is explained by the formation of a WO_3 layer in the film, seen in Raman spectroscopy, which protects the exposed surface against electrolyte attacks. However, when Ti is included in the samples, a large reduction in corrosion resistance is observed, even at significantly lower concentrations and in pure samples, as is the case of the WS_2-$Ti_{0.25}$ W/cm^2 and WS_2-$Ti_{0.5}$ W/cm^2 samples, respectively. This behavior is caused by increased stress and recrystallization processes generated as a result of the inclusion of Ti in the WS_2 structure [6,14], creating active sites and film defects that in turn increase the strength of electrolyte attacks [30]. However, when the material contains a higher Ti concentration (WS_2-$Ti_{0.75}$), the observed increase in corrosion resistance was even superior to that of the pure sample. The corrosion resistance increases along with Ti content in the material, due to structural rearrangement at these Ti percentages [14], generating a film with few defects and greater density [12]. In addition, the characteristic behavior of Ti possibly allows the formation of a thin layer of TiO_2, which helps inhibit the attack of the solution and improves the corrosion resistance [31].

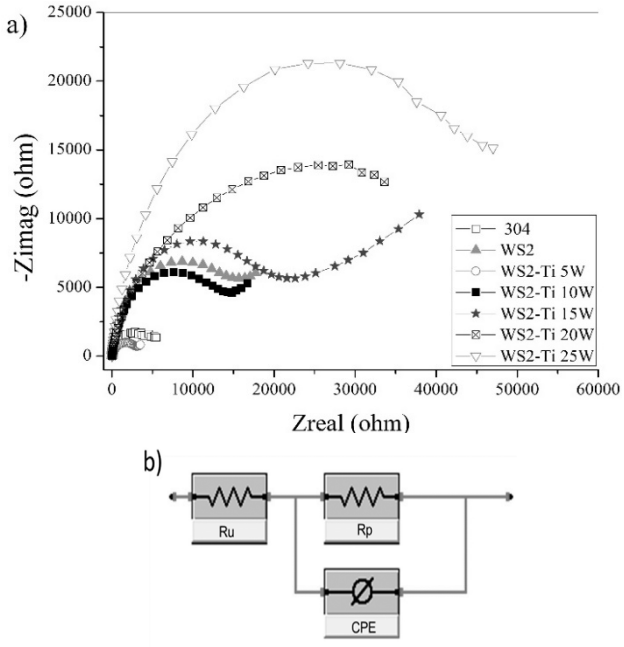

Figure 5. a) Nyquist diagram of steel, WS_2 and WS_2-Ti (x) b) equivalent circuit.
Source: The authors

3. Conclusions

The μ-Raman spectroscopy results for the WS_2 sample showed major bands corresponding to the A_{1g} and E_{2g} modes. Additionally, bands corresponding to WO_3 indicating the formation of oxides on the surface of the WS_2 were observed. When the material is doped structural changes are reflected in the elimination of the main bands; this is caused by the distortion of Ti included in the lattice, preventing free movement of tungsten and sulfur, or because of a phase change.

Scratch test results showed changes in the tribological properties of the material as a result of doping. Furthermore, increasing Ti contents in the samples resulted in progressive failures of brittle materials. A decrease in critical load values following doping was observed because the maximum value of doped samples (WS_2-$Ti_{1.25}$ *Lc* = 15 N) was lower compared to that of the pure sample (*Lc* = 18 N).

Electrochemical impedance spectroscopy (EIS) results indicated an increase in corrosion resistance of the substrate with the addition of a WS_2 layer. The presence of WO_3 on the surface, evidenced by Raman results, contributes to protection from the solution. At higher Ti concentration levels, there was a considerable increase in corrosion resistance due to recrystallization processes in the material, increased material densification, reduction in the number of defects, and the number of active sites in the film, which helped avoid solution-related attacks. Furthermore, Ti was capable of forming an oxide layer helped to protect against corrosion.

Acknowledgments

The authors gratefully acknowledge the financial support of the Facultad de Ciencias Exactas y Naturales of the Universidad Nacional de Colombia – Sede Manizales and the Dirección Nacional de Investigaciones of the Universidad Nacional de Colombia – sede Manizales (DIMA) during the course of this research under projects 36736 and 35936.

References

[1] Shen, B., Chen, S., Chen, Y. and Fanghong, S., Enhancement on the tribological performance of diamond films by utilizing graphene coating as a solid lubricant. Surface and Coatings Technology, 311, pp. 35-45, 2017. DOI: 10.1016/j.surfcoat.2016.12.094

[2] Gunda, R.K. and Narala, S.K.R., Tribological studies to analyze the effect of solid lubricant particle size on friction and wear behavior of

Ti-6Al-4V alloy. Surface and Coatings Technology, 308, pp. 203-212, 2016. DOI: 10.1016/j.surfcoat.2016.06.092
[3] Singh, H., Mutyala, K.C., Evans, R.D. and Doll, L., An investigation of material and tribological properties of Sb2O3/Au-doped MoS2 solid lubricant films under sliding and rolling contact in different environments. Surface and Coatings Technology, 284, pp. 281-289, 2015. DOI: 10.1016/j.surfcoat.2015.05.049
[4] Viat, A., Fouvry, S., De barros-Bouchet, M.I. and Pin, L., Influence of carbon-based solid lubricant on fretting wear response for alumina-based ceramics versus cobalt superalloy contact. Surface and Coatings Technology, 284, pp. 327-333, 2015. DOI: 10.1016/j.surfcoat.2015.07.043
[5] Hilton, M.R. and Fleischauer, P.D., Applications of solid lubricant films in spacecraft. Surface and Coatings Technology, 54-55(2), pp. 435-441, 1992. DOI: 10.1016/S0257-8972(07)80062-4
[6] Scharf, T.W., Rajendran, A., Banerjee, R. and Sequeda, F., Growth structure and friction behavior of titanium doped tungsten disulphide (Ti-WS2) nanocomposite thin films. Thin Solid Films, 517(19), pp. 5666-5675, 2009. DOI: 10.1016/j.tsf.2009.02.103
[7] Scharf, T.W., Prasad, S.V., Dugger, M.T., Kotula, P.G., Goeke, R.S. and Grubbs, R.K., Growth, structure, and tribological behavior of atomic layer-deposited tungsten disulphide solid lubricant coatings with applications to MEMS. Acta Materalia, 54(18), pp. 4731-4743, 2006. DOI: 10.1016/j.actamat.2006.06.009
[8] Muratore, C. and Voevodin, A.A., Chameleon coatings: adaptive surfaces to reduce friction and wear in extreme environments. Annual Review Materials Research, 39, pp. 297-324, 2009. DOI: 10.1146/annurev-matsci-082908-145259
[9] An, V., Bozheyev, F., Richecoeur, F. and Irtegov, Y., Synthesis and characterization of nanolamellar tungsten and molybdenum disulfides. Materials Letters, 65(15-16), pp. 2381-2383, 2011. DOI: 10.1016/j.matlet.2011.05.048
[10] Zhang, X., Qiao, L., Chai, L., Xu, J., Shi, L. and Wang, P., Structural, mechanical and tribological properties of Mo–S–N solid lubricant films. Surface and Coatings Technology, 296, pp. 185-191, 2016. DOI: 10.1016/j.surfcoat.2016.04.040
[11] Polcar, T. and Cavaleiro, A., Review on self-lubricant transition metal dichalcogenide nanocomposite coatings alloyed with carbon. Surface and Coatings Technology, 206(4), pp. 686-695, 2011. DOI: 10.1016/j.surfcoat.2011.03.004
[12] Nossa, A. and Cavaleiro, A., Mechanical behaviour of W–S–N and W–S–C sputtered coatings deposited with a Ti interlayer. Surface and Coatings Technology, 163-164(4), pp. 552-560, 2003. DOI: 0.1016/S0257-8972(02)00622-9
[13] Zheng, X.H., Tu, J.P., Lai, D.M., Peng, S.M., Gu, B. and Hu, S.B., Microstructure and tribological behavior of WS2 – Ag composite films deposited by RF magnetron sputtering. Thin Solid Films, 516(16), pp. 5404-5408, 2008. DOI: 0.1016/j.tsf.2007.07.102
[14] De la Roche, J., Gonzalez, J.M., Restrepo-Parra, E. and Sequeda, F., Structure and properties of titanium doped tungsten disulfide thin films produced via the magnetron co-sputtering dc technique. Matéria, 21(2), pp. 461-469, 2016. DOI: 0.1590/S1517-707620160002.0043
[15] Renevier, N.M., Fox, V.C., Teer, D.G. and Hampshire, J., Coating characteristics and tribological properties of sputter-deposited MoS2/metal composite coatings deposited by closed field unbalanced magnetron sputter ion plating. Surface and Coatings Technology, 127, pp. 24-37, 2000. DOI: 10.1016/S0257-8972(00)00538-7
[16] Efeoglu, I., Baran, Ö., Yetim, F. and Altintasl, S., Tribological characteristics of MoS2–Nb solid lubricant film in different tribo-test conditions. Surface and Coatings Technology, 203, pp. 766-770, 2008. DOI: 10.1016/j.surfcoat.2008.08.048
[17] Seikh, A.H., Baig, M., Ammar, H.A. and Alam, M.A., The influence of transition metals addition on the corrosion resistance of nanocrystalline al alloys produced by mechanical alloying. Metals, 6, pp. 140-144, 2016. DOI: 10.3390/met6060140
[18] Banerjee, T. and Chattopadhyay, A.K., Structural, mechanical and tribological properties of pulsed DC magnetron sputtered TiN–WSx/TiN bilayer coating. Surface and Coatings Technology, 282, pp. 24-35, 2015. DOI: 10.1016/j.surfcoat.2015.10.011
[19] Carmalt, C.J., Parkin, I.P. and Peters, E.S., Atmospheric pressure chemical vapor deposition of WS2 thin films on glass. Polyhedron, 22(11), pp. 1499-1505, 2003. DOI: 10.1016/S0277-5387(03)00194-3
[20] Tagtstrom, P. and Jansson, U., Chemical vapor deposition of epitaxial WO3 films. Thin Solid Films, 352(1-2), pp. 107-113, 1999. DOI: 10.1016/S0040-6090(99)00379-X
[21] Díaz-Reyes, J., Dorantes-García, V., Pérez-Benítez, A. and Balderas-López, J.A., Obtaining of films of tungsten trioxide (WO3) by resistive heating of a tungsten filament. Superficies y Vacío, 21(2), pp. 12-17, 2008.
[22] Ramana, C.V., Utsunomiya, S., Ewing, R.C., Julien, C.M. and Becker, U., Structural stability and phase transitions in WO3 thin films. Journal Physical Chemistry B, 110(21), pp. 10430-10435, 2006. DOI: 10.1021/jp056664i
[23] Bertrand, P.A., Orientation of rf-sputter-deposited MoS2 films. Journal of Materials Research, 4(1), pp. 180-184, 1989. DOI: 10.1557/JMR.1989.0180
[24] Genut, M., Margulis, L., Tenne, R. and Hodes, G., Effect of substrate on growth of WS2 thin films. Thin Solid Films, 219(1-2), pp. 30-36, 1992. DOI: 10.1016/0040-6090(92)90720-V
[25] Colomban, P. and Slodczyk, A., Raman intensity: An important tool to study the structure and phase transitions of amorphous/crystalline materials. Optical Materials, 31(12), pp. 1759–1763, 2009. DOI: 10.1016/j.optmat.2008.12.030
[26] ASTM C 1624 – 05 Standard test method for adhesion strength and mechanical failure modes of ceramic coatings by quantitative single point scratch testing
[27] Balagna, C., Faga, M.G. and Spriano, S., Tantalum-based multilayer coating on cobalt alloys in total hip and knee replacement. Materials Science Engineering C, 32(4), pp. 887-895, 2012. DOI: 10.1016/j.msec.2012.02.007
[28] Katayama, H. and Kuroda, S., Long-term atmospheric corrosion properties of thermally sprayed Zn, Al and Zn–Al coatings exposed in a coastal area. Corrosion Science, 76, pp. 35-41, 2013. DOI: 10.1016/j.corsci.2013.05.021
[29] Orazem, M.E. and Tribollet, B., Electrochemical impedance spectroscopy. John Wiley & Sons, 2011.
[30] Ahn, S.H., Lee, J.H., Kim, J.G. and Han, J.G., Localized corrosion mechanisms of the multilayered coatings related to growth defects. Surface and Coatings Technology, 177-178, pp. 638-644, 2004. DOI: 10.1016/S0257-8972(03)00939-3
[31] Revie, W.R. and Uhlig, H.H., Corrosion and corrosion control, 4th ed., New Jersey, John Wiley & Sons, Inc, 2008. DOI: 10.1002/9780470277270

J. De la Roche-Yepes, is BSc. in Materials Science Eng., in 2010, MSc. in Physics, in 2014. Awarded twice with COLCIENCIAS' Scholarship for young researchers. Worked in projects involving thin-film deposition for industrial applications, vacuum systems assembly and plasma-assisted techniques (PVD and CVD). He is currently a PhD candidate in Materials Science Engineering at the Universidad Nacional de Colombia.
ORCID: 0000-0003-3131-3096

J.M. González, is BSc. in Physics Eng. in 2005, MSc. in Physics in 2007, PhD in Materials Engineering in 2014. His research interests involve surface engineering with emphasis in coating deposition by PVD, CVD, projection, electrolytic techniques and other superficial treatments such as ionic implantation, heat treatments, science infrastructure administration and industrial equipment development. At present he leads the TECNOACADEMIA program in Centro ASTIN-SENA in Cali, Colombia.
ORCID: 0000-0003-0659-4156

E. Restrepo-Parra, is BSc. in Electrical Eng. in 1990 from the Universidad Tecnológica de Pereira, Colombia, MSc. in Physics in 2000, PhD in Engineering – Automatization in 2009, both from the Universidad Nacional de Colombia in Manizales, Colombia. From 1991 to 1995, she worked in the Colombian electrical sector and from 1996 onwards for the Universidad Nacional de Colombia. Currently, she is a senior professor at the Physics and Chemistry Department, in the Facultad de Ciencias Exactas y Naturales, Universidad Nacional de Colombia – Sede Manizales. Her research interests include: simulation and modeling of properties of materials by several methods; processing of materials by plasma assisted techniques; and characterization of materials. She is currently Laboratories Director of Universidad Nacional de Colombia – Sede Manizales.
ORCID: 0000-0002-1734-1173

H. Sanchez-Sthepa, is BSc. in Metallurgical Eng., from the Universidad Industrial de Santander, Colombia, MSc. in Physical Sciences, PhD in Physics, from the Universidad del Valle, Cali, Colombia. Specialized in powder metallurgy, mechanical alloys, hard coatings and materials science. Currently full-time professor at the Universidad del Valle, in the Faculty of Engineering; is research director in the group "Recubrimientos Duros y Aplicaciones Industriales-RDAI".
ORCID: 0000-0002-6574-0005